**Fachtagung "Experimentelle Strömungsmechanik"**
7.–9. September 2021, Bremen

# Verwendung der Wollaston-Scherinterferometrie zur Untersuchung des Brechungsindexgradienten in einem differentiell beheizten Ringspalt

## Utilizing Wollaston shearing interferometry to investigate the refractive index gradient in a differentially heated annulus

**Erdogdu[1], A.O., Szabo[1], P.S.B., Carter[2], R., Gevrek[1], M.-E., Haun[1], P., Zaussinger[3], F., Schulze[1], B., Meier[1], M., Egbers[1], Ch.**
[1]Department of Aerodynamics and Fluid Mechanics, BTU Cottbus-Senftenberg, Cottbus, Germany
[2]Institute of Photonics and Quantum Sciences, Heriot-Watt University, Edinburgh, United Kingdom
[3]Faculty CB, University of Applied Sciences Mittweida, Mittweida, Germany

**Schlagworte:** Wollaston-Scher-Interferometrie, Freie Konvektion, Differentiell geheizter Ringspalt
**Key words:** Wollaston shearing interferometry, natural convection, differentially heated annulus

### Abstract
Natural convection is studied in a differentially heated annulus with its axis aligned in the horizontal direction to induced the so called *"crescent shaped pattern"* of two axisymmetric counter-rotating convection cells. To investigate this particular temperature and flow pattern the Wollaston shearing interferometry is utilised which serves as the measurement system for the AtmoFlow project, a spherical shell that is designed to investigate atmospheric flow fields on the ISS planned to be launched in 2024. To be able to understand the measured flow fields in the sphere, ground experiments are carried out with the differentially heated annulus. For the sake of simplicity, the system is categorised in three classes, the initial isothermal state where only artificial fringes are measured, the conduction case with symmetric fringes and the convective state where fringes align with the crescent shaped convection pattern.

### Introduction
Convection in spherical shells and annuli have proven to be useful geometries to study large scale convection such as stellar interiors or atmospheres (Früh et al. 2017, 2020; Szabo et al. 2020, 2021a,b; Zaussinger et al. 2020). One of the recent examples is the GeoFlow project, a spherical shell with an electrically induced central force field to study a planets inner core (Zaussinger et al. 2018, 2020). This simple model was studied for several years on the International Space Station (ISS) providing microgravity conditions to reveal the essential insight into a liquid core, solid core and mantel convection such as is on Earth. The successor, the AtmoFlow space project, planned to be launched in 2024 is aimed to investigate zonal convection in a spherical gap geometry to gain a greater understanding of atmospheric flow e.g. for planetary systems with deep atmospheres ( Zaussinger et al. 2019; Szabo et al. 2020; Haun 2021). While the experiments carried out on the ISS, several health and safety restrictions have to be considered. As only non-invasive measurements techniques fulfil the requirements for electrical safety, the choice was made to use a density-based technique to capture the evolving temperature fields inside the spherical shell by use of an interferometry system. Alongside the manufacturing of the AtmoFlow experiment a series of ground experiments are performed to first validate the measurement technique based on Wollaston

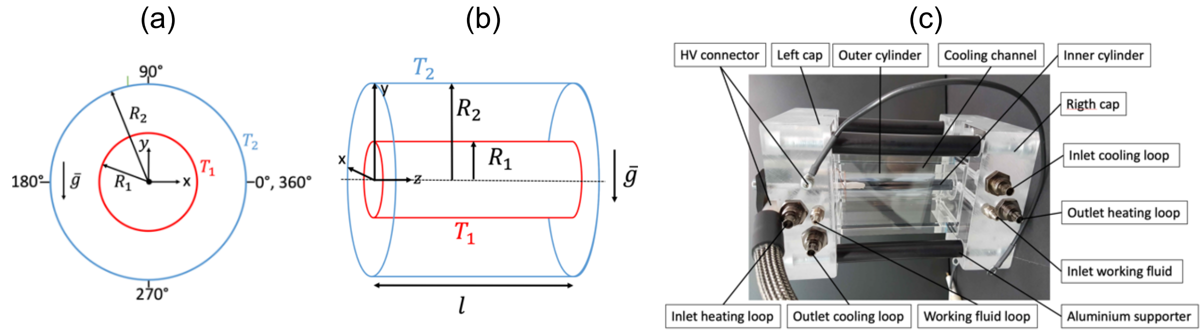


**Figure 1: Sketch of experiment cell in (a) and (b) with boundary conditions and (c) physically manufactured cavity.**

shearing interferometry (WSI) and second to be able to reconstruct the flow and temperature fields by using recorded interferometry images of a differentially heated annulus. The expected outcome should improve the data post-processing of the AtmoFlow space experiment and provide a better understanding of the geophysical and metrological insight of planetary atmospheres.

The system for testing the Wollaston shearing interferometry consisted of a differentially heated annuls with the z-axis aligned in the horizontal direction, see section Experiment setup. This configuration enables study of a stationary convective pattern the so-called *“crescent shaped pattern”* (Powe et al. 1969; Yoo 1996) at small Rayleigh numbers where hot fluid ascends from the inner heated cylinder towards the outer cylinder to produce a mushroom shaped structure. The hot fluid is cooled at the outer cylinder where it descends towards the bottom of the annulus to form two convection cells and thus the crescent shaped pattern. Using such a simple system enables detection of small variations in the refractive index of the fluid by Wollaston shearing interferometry which is proportional to the fluid’s density and temperature. A detailed explanation of the measurement and experiment setup is given in the following section followed by the presentation of recorded interference images. An interpretation of the results follows in the discussion section and is concluded at the end.

## Experiment setup

The experiment consists of: an experiment cell; a differentially heated cylindrical annulus; and the measurement and data acquisition system. The experiment is made out of two concentric cylinders of radius $R_1$ and $R_2$ and aligned with its z-axis in horizontal direction. Boundary conditions are displayed in Figure 1 (a) and (b) together with the physically built system in (c). A full description of the experiment cell, material properties and the confined working fluid between both cylinders is given in (Meier et al. 2018). The fluid is heated at the inner and outer

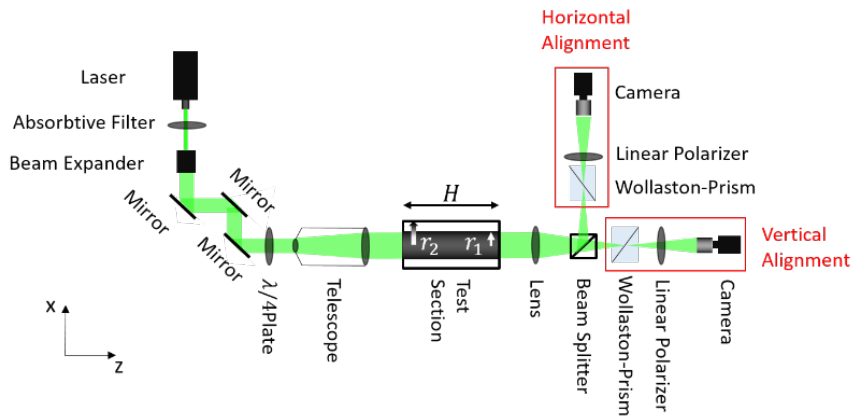


**Figure 2: Experimental setup of the measurement equipment**

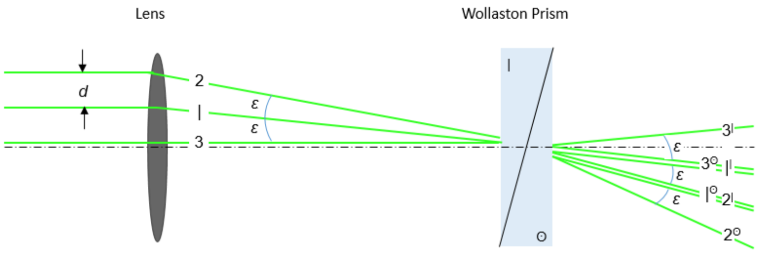


**Figure 3: Beam separation within the Wollaston Prism** (Tropea et al. 2007)

cylinder with $T_1$ and $T_2$, respectively where $T_1 = T_2 + \Delta T$ to induce natural convection within the cavity. For the experiment three different temperature differences of $1.5$ K, $2.5$ K and $5$ K are recorded.

To capture the evolving temperature distribution inside the cavity a density-based technique is used, Wollaston shearing interferometry, displayed in Figure 2. The system is based on a plane polarized laser beam with 2 mm diameter at the aperture and is sent through a beam expander where two adjustable mirrors are used to provide beam path alignment control as needed. A third mirror directs the beam into a $\lambda/4$-plate to convert the plane polarized light into circularly polarized light. Prior to the test section a second beam expander increases the beam size to about 60 mm FWHM in diameter to pass it through the differentially heated cylindrical annulus. After the test section the beam is focussed with a lens into a Wollaston prism where the beam is split into two linearly polarised rays with orthogonal polarization, relative as indicated in Figure 3. To understand the principle, we only show three circular polarized rays focused into the Wollaston prism that separates each ray into coincident plane polarized rays relative to each other with orthogonal polarization. Interference of the two rays is established with a linear polarizer rotated by 45° with respect to the Wollaston prism. To capture the resulting interference a commercially available camera system manufactured by Imagine Source with a 50 mm lens is used to image the beam onto the camera's sensor.

It has to be noted that Wollaston shearing interferometry is able to measure in two different modes, infinite fringe width (IFW) and finite fringe width (FFW). The difference between these modes is achieved by shifting the Wollaston prism into or out of focus. The visual difference is noted e.g., by the FFW where parallelly aligned fringes become visible. The number of visible fringes depend on the distance of the Wollaston prism to the focal point. If the Wollaston prism is in focus (IFW), no fringes should be visible as long as the test section's refractive index is undisturbed and does not show any alternations.

For this study the setup used the IFW mode where the Wollaston prism is in focus. An example of the adjustment is given in Figure 4 (a) displaying an interferometry image of the measured refractive index gradient within and around a steady candle flame in both vertical (a) and horizontal direction (b). To capture the reflective index gradient correctly aligning the polarizer to the Wollaston is crucial. If one of both components is not correctly aligned the polarizer may only pass one of the two polarisation states separated by the Wollaston prism.

(a) (b)

**Figure 4: IFW interferograms of a steady candle flame in (a) and (b) with the difference that a second Wollaston prism is rotated 90° to capture the orthogonal refractive index gradient. The combination of the two images thus provides both gradients.**



GALA e.V., Karlsruhe, Germany, ISBN 978-3-9816764-7-1

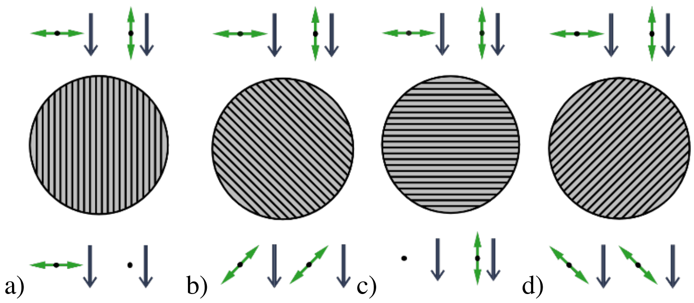


**Figure 5: Effect of a linear polarizer on 2 orthogonally polarized coaxial existing incident beams with the linear polarizer rotations of 0° (a), 45° (b), 90° (c) and 135° (d).**

An example of polarization directions is given in Figure 5. This polarization issue potentially causes confusion between IFW mode and a system which permits only one polarisation mode to pass; in both cases no fringes are visible. As long as the relative angle between the Wollaston prism and the linear polarizer is 45°, the system will measure a component of the refractive index gradient which is normal to the fringes in either FFW or IFW mode (Carlomagno and Rapillo 1986). Using a beam splitter as depicted in Figure 2 enables to capture of both index gradients at the same time provided the Wollaston prisms and associated polarizers are orthogonally rotated to one another. These alignments are labelled as horizontal and vertical.

Correct adjustment of the system can be achieved depending on the expected fluctuations of the system e.g., a candle benchmark test where a steady flame causes natural convection. The system is first configurated by adjusting the Wollaston prism to measure one refractive index gradient and moved out of focus such that a regular FFW fringe pattern becomes visible. By rotating the Wollaston prism together with the polarizer, the fringe pattern can be aligned in vertical or horizontal direction to be able to distinguish between the two refractive index gradients $\partial n/\partial x$ and $\partial n/\partial y$ in a 2D-plane referred as the *"double component refractive index gradient"*. After this process the Wollaston prisms are moved carefully back into focus to measure with the IFW mode such that inference patterns can arise through a change in the refractive index gradient.

**Image post-processing**

While the interference images show the region of interest and also the surroundings, only the cylindrical gap region is post-processed. A mask is created by defining three points on the outer cylinder defining the outer boundary and is used to subtract regions that are not of interest. By using triangulation, the meaningless regions are set to not a value and thus only the cylindrical gap is postprocessed and converted from RGB values into a grey scale to provide a grey level ($GL$) which is plotted using a grey scale map.

**Results**

In this section we present the recorded and post-processed interferometry images for both refractive index gradients. Their interpretation and physical meaning are given in the following discussion section.

We first present the initial state of the system in Figure 6 and Figure 7 for each refractive index direction defined as the vertical and horizontal component for each run at $t = 0$ s where no thermal forcing is present. This provides an indication of artificial fringes caused by the imperfect annulus with respect to geometrical and material properties that are difficult to avoid. The first panel in Figure 6 and Figure 7 (a, f, k) indicates such artificial fringes expected to be caused by the birefringence properties of the acrylic glass (PMMA) material of the annulus containment. At $t = 30$ s no further fringes appear and the system remains still in its isothermal state as seen in Figure 6 and Figure 7 (b, g, l). At about $t = 120$ s a relatively regular fringe pattern appears for the cases (c) and (h) in both figures. The interferometry images show an

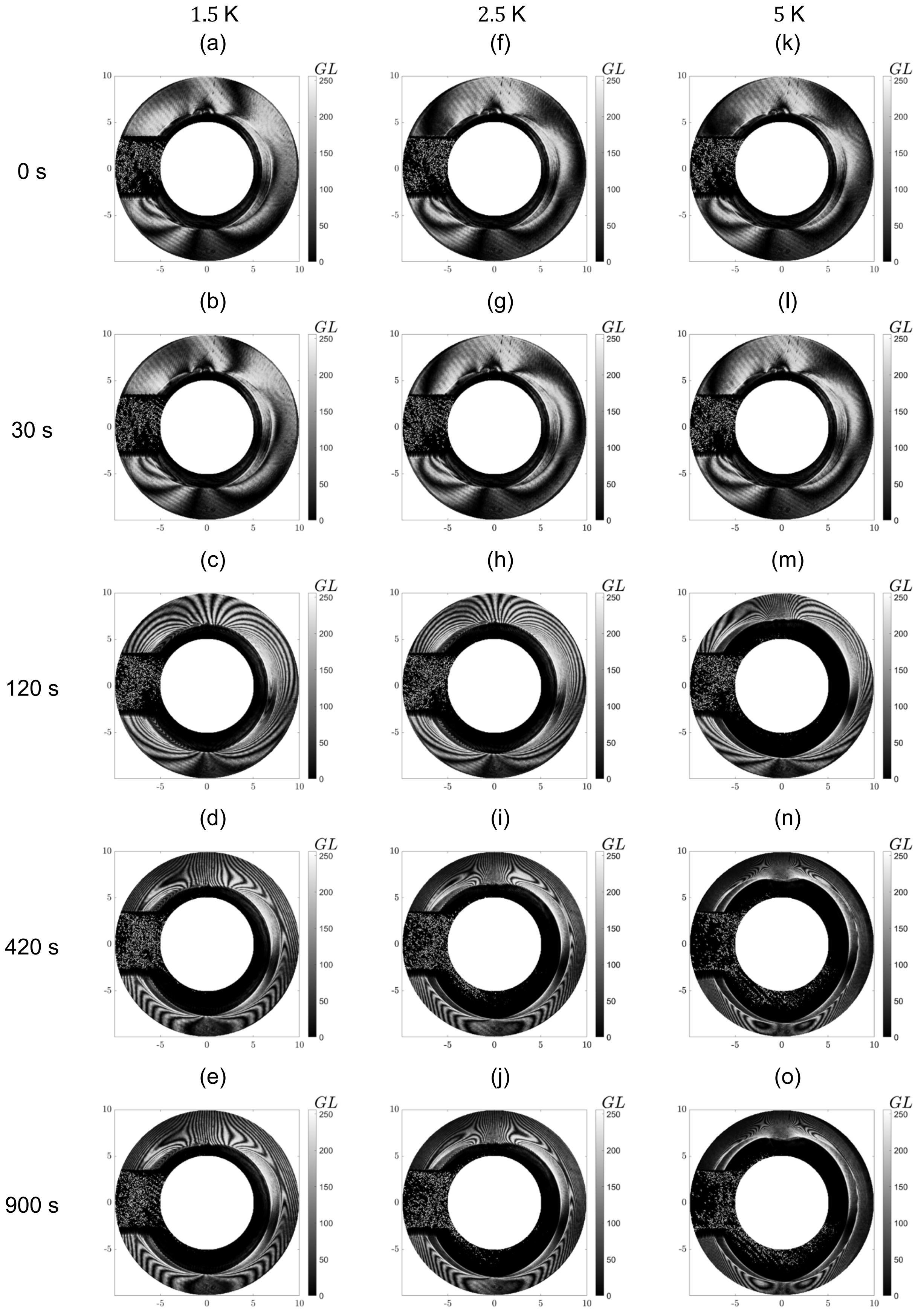


**Figure 6: Recorded interference images at different $\Delta T$ with vertical Wollaston alignment.**

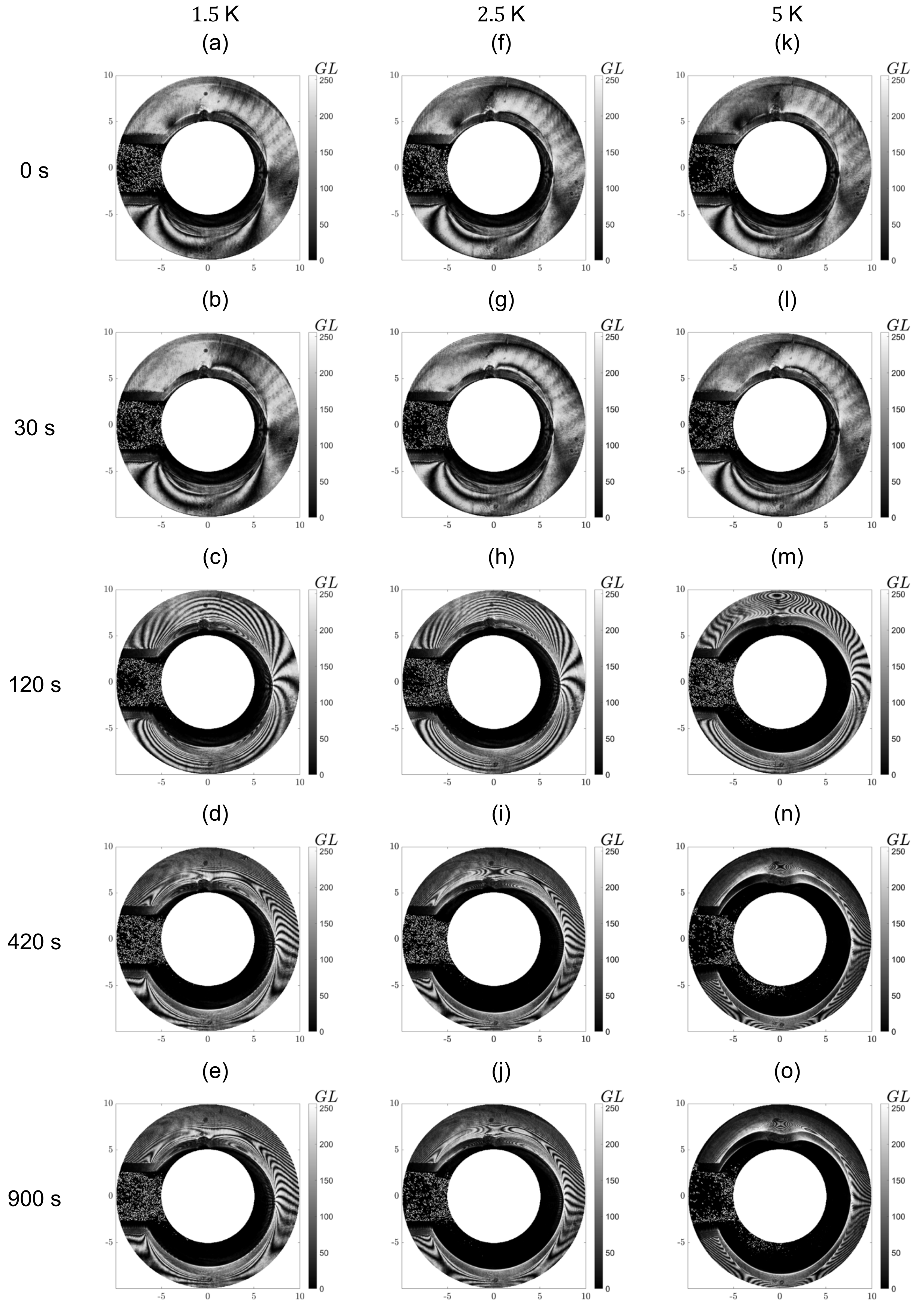


**Figure 7: Recorded interference images at different $\Delta T$ with horizontal Wollaston alignment.**

equivalent pattern; however these are rotated by 90° when comparing the vertical and horizontal alignment with one another. This is different for case (m) where fringes seem to have stronger local variation with larger fringe frequency that are separated by a smaller distance. In general, an increase in fringe frequency is noted when the temperature difference is increased see (n) and (o) compared to (i) and (j) or (d) and (e). A similar effect is noted when the system has not yet equilibrated to the stationary crescent shaped convection pattern see (a-e) in both Figures. In fact, the system is still in a transitional state from the isothermal state to the quasi-stationary state where the fringe distance decreases and fringe frequency increases with temperature.

**Discussion**

The physical interpretation of the recorded refractive index refers to a non-isothermal perturbation of the system as $n \sim \rho \sim T$. However, as already indicated in the result section fringes appear in Figure 6 and Figure 7 (a, f, k, b, g, l) respectively. Such large fringes are referred as artificial fringes and relate to the manufacturing of the annulus material containment made out of PMMA that is known to create shearing effects when the system is under mechanical stress e.g., by bolt connections. The shape of such artificial fringes may be arbitrary and depend on the system that is measured. To classify the fringe pattern, we adopt the first classification of the "*initial fringe pattern"* prior to measurements.

In the presence of non-isothermal perturbation for example by causing a temperature difference between the inner and outer cylinder such initial fringe patterns seem to disappear as local variations in the refractive index dominate. The fringe patterns thus generated refer now to the evolving non-isothermal perturbation see for example Figure 6 and Figure 7 (c) and (h) respectively. This first sign of a regular pattern is found where fringes extend from the top ($\theta = 90°$) towards the bottom ($\theta = 270°$) for the vertical Wollaston alignment and from left ($\theta = 90°$) towards the right ($\theta = 180°$) in the horizontal Wollaston alignment with an axisymmetric shape. However, the structure does not follow the expected crescent shaped pattern yet as conduction is one transition phase before convection sets in and equilibrates to a quasi-stationary flow. The shape of regular fringes is interpreted as the conduction case and is the second classification of the system after the initial state and referred as the *"conduction fringe pattern"*.

The third classification considers the recorded crescent shape pattern where convection is present. This is clearly visible where the fringe structure follows the convection pattern very closely in vertical and horizontal Wollaston alignment presenting the refractive index differences caused by the established temperature field. While the crescent shape pattern is quasi-stationary, the shape does not vary in time after the equilibration process and thus can be well defined by the convection pattern in Figure 6 and Figure 7 (n, o, I, j, d, e), respectively. This classification is named the *"convective fringe pattern"*. It has to be noted at the inner boundary the laser beam is refracted towards the outer cylinder and a black ring around the inner cylinder is established. This effect is well known also for the shadowgraph measurements conducted in the same system (see, Meier et al. 2018).

**Conclusion**

In this study natural convection inside a differentially heated annulus with its z-axis aligned in horizontal direction perpendicular to the Earth's gravity was studied experimentally. The purpose of this experiment served to obtain an indication of the capability of the Wollaston shearing interferometry for the measurement of flow fields within the AtmoFlow space experiment, an experiment that is to be launched in 2024 on the ISS to investigate large scale convection of planetary atmospheres. During the experimental investigation a common convection structure, the *crescent shaped pattern*, a quasi-stationary pattern that has equilibrated in time, was investigated. This served to classify the recoded into three categories.

The first fringe classification is the *initial fringe pattern* caused by the experiment cell where no thermal forcing is present. Thus, the fringes are refereed as artificial fringes, caused for example by the manufacturing process or mechanical strain. The second classification considered the heat transport by conduction where a regular fringe pattern is observed. This case was classified as the *conduction fringe pattern*. The third and last classification considered the expected *crescent shaped pattern* of two counter rolling convection cells that are axisymmetric. The interference images clearly showed the pattern by following the refractive index differences that is proportional to the fluid's density and temperature. The fringe pattern was classified as the *convective fringe pattern*. To summarise, this study has demonstrated an ability to measure conductive and convective flow fields by utilizing Wollaston shearing interferometry and an ability to interpret the fringes in context of the expected fringe pattern classified in three categories.

**Acknowledgements**
The project AtmoFlow is supported by the BMWi via the German Space Administration of the Deutsches Zentrum für Luft und Raumfahrt (DLR) with grant no. 50WP1709, 50WP1809 and 50WM2141.

**References**

**Carlomagno, G.M., Rapillo, A., 1986:** "A Wollaston Prism Interferometer Implemented with a Digitizer", Experiments in Fluids, Vol. 4, pp. 322–36

**Früh, W.-G., Szabo, P.S.B., Seelig T., Hoff M., Egbers C. 2017:** "Identifying Representative Shapes in Fields of Temperature Spectra in Vacillating Baroclinic Waves", EGU General Assembly 2020

**Früh, W.-G., Szabo, P.S.B., Egbers, C., Harlander, U., 2020:** "Locating Sources of Variability in the Transition to Structural Vacillation in the Baroclinic Annulus" EGU General Assembly 2020

**Haun, P., Zaussinger, F., Szabo, P.S.B., Egbers, C., 2021:** "AtmoFlow - Investigating planetary fluid flow on the International Space Station", EGU General Assembly 2021

**Meier, M., Jongmanns, M., Meyer, A., Seelig, T., Egbers, C., Mutabazi, I., 2018:** "Flow Pattern and Heat Transfer in a Cylindrical Annulus Under 1 g and Low-g Conditions: Experiments." Microgravity Science and Technology, Vol.30, No. 5, pp. 699–712

**Powe, R.E., Carley, C.T., Bishop E.H. 1969:** "Free Convective Flow Patterns in Cylindrical Annuli." Journal of Heat Transfer Vol. 91, No. 3, pp. 310–14

**Szabo, P.S.B., Zaussinger, F., Haun, P., Froitzheim, A., Carter, R., Travnikov, V., Meier, M., Egbers, C., 2020:** "Complementary Numerical and Experimental Study in the Baroclinic Annulus for the Microgravity Experiment AtmoFlow." EGU General Assembly 2020, Vienna.

**Szabo, P.S.B., Früh, W.-G., 2018:** "Using Magnetic Fluids to Model Convection of Planetary or Stellar Interiors in Laboratory Scale." PAMM, Vol.18, No. 1

**Szabo, P.S.B., Früh, W.-G. 2021a:** "Thermomagnetic Convection in a Differentially Heated Rotating Annulus with Central Force Field." PAMM, Vol. 21, No. 1, pp.1–2

**Szabo, P.S.B., Früh, W.-G. 2021b:** "Convective pattern formation in a thermally heated rotating annulus with magnetic central force field" EGU General Assembly 2021

**Tropea, C., Yarin, A.L., Foss, J.F., 2007:** "Handbook of Experimental Fluid Mechanics", Springer-Verlag Berlin Heidelberg

**Yoo, J.-S., 1996:** "Dual Steady Solutions in Natural Convection between Horizontal Concentric Cylinders." International Journal of Heat and Fluid Flow, Vol.17, No. 6, pp. 587–593

**Zaussinger, F., Haun, P., Neben, M., Seelig, T., Travnikov, V., Egbers, C., and Yoshikawa, H., Mutabazi, I., 2018:** "Dielectrically Driven Convection in Spherical Gap Geometry." Phys. Rev. Fluids, Vol. 3, No. 9, pp. 93501

**Zaussinger, F., Canfield, P., Froitzheim, A., Travnikov, V., Haun, P., Meier, M., Meyer, A., Driebe, T., Egbers, C., 2019:** "AtmoFlow - Investigation of Atmospheric-like Fluid Flows under Micro-Gravity Conditions." Microgravity Science and Technology, Vol. 31, pp. 569–587

**Zaussinger, F., Haun, P., Szabo, P.S.B., Travnikov, V., Al Kawwas, M., Egbers, Ch., 2020:** "Rotating Spherical Gap Convection in the GeoFlow International Space Station (ISS) Experiment" Phys. Rev. Fluids, Vol. 5, pp. 063502


GALA e.V., Karlsruhe, Germany, ISBN 978-3-9816764-7-1